Particuology xxx (2016) xxx–xxx

Contents lists available at ScienceDirect

Particuology

journal homepage: www.elsevier.com/locate/partic

Invited paper

Validation of surface coating with nanoparticles to improve the flowability of fine cohesive powders

Xiaolin Zhu[a,b], Qiang Zhang[a,*], Cang Huang[a], Yao Wang[a], Chaohe Yang[b], Fei Wei[a]

[a] Beijing Key Laboratory of Green Chemical Reaction Engineering and Technology, Department of Chemical Engineering, Tsinghua University, Beijing 100084, China
[b] State Key Laboratory of Heavy Oil Processing, China University of Petroleum, Qingdao 266580, China

ARTICLE INFO

Article history:
Received 3 March 2016
Received in revised form 5 June 2016
Accepted 28 September 2016
Available online xxx

Keywords:
Fine cohesive powders
Fluidization
Nanoparticle coating
Interparticle adhesion force
Flowability prediction

ABSTRACT

Fluidization of fine cohesive powders is seriously restricted by the strong interparticle cohesion. The rational combination of nanoparticles with fine cohesive powders is expected to obtain composite particles with improved flowability. In this work, we firstly reviewed the sandwich and three-point contact models regarding the fundamental principles of nano-additives in reducing cohesiveness. Based on these previous models, the effects of the size of nanoparticles, their agglomeration and coverage on the surface of cohesive powders in reducing interparticle forces were theoretically analyzed. To validate the theory effectiveness for the irregularly shaped cohesive powders, an extreme case of cubic powders coated with silica nanoparticles was fabricated, and the flowability of the composite particles was determined experimentally. Ultimately, based on force balance of a single particle, a semi-theoretical criterion for predicting the fluidization behavior of coated powders was developed to guide the practical applications of improving the flowability of cohesive powders through structural design and modulation.

Introduction

The flow behavior of particles depends on their intrinsic structures and morphologies. Based on the particle size and the density difference between solid material and fluidizing medium, Geldart has classified the powders into four groups: A, B, C, and D (Geldart, 1973). Group C powders, namely fine cohesive particles, have been broadly applied in pharmaceutical, food, chemical, and cosmetics industries. However, the strong interparticle adhesion force of these fine cohesive powders induces intense particle agglomeration, and further restricts their smooth fluidization and facile transportation (Wang, Zhu, & Beeckmans, 2000; Wang, Cheng, Jin, & Bi, 2007). Consequently, the handling of cohesive powders becomes a great scientific challenge and urgent technological issue for their bulk applications.

Group C cohesive powders, when subjected to fluidizing gas, tend to form cracks, channels, or even lift as slugs. Although agglomerate fluidization may be possible in some cases, due to the instability of the formed agglomerates, the bed preferentially dies in partial fluidization or even complete defluidization (van Ommen, Valverde, & Pfeffer, 2012). To improve the flow quality of cohesive powders, two types of methods in terms of different mechanisms have been explored. The first approach intends to overcome the interparticle interactions by introducing external excitation, such as mechanical vibration (Kaliyaperumal, Barghi, Briens, Rohani, & Zhu, 2011; Nam, Pfeffer, Dave, & Sundaresan, 2004; Xu & Zhu, 2005, 2006), acoustic wave (Guo, Liu, Shen, Yan, & Jia, 2006; Liu, Guo, & Chen, 2007; Xu, Cheng, & Zhu, 2006), magnetic stirring (Yu, Dave, Zhu, Quevedo, & Pfeffer, 2005), rotating drum (Huang, Zhang, & Zhu, 2009; Huang, Zhang, & Zhu, 2010b), electric field disturbance (Lepek, Valverde, Pfeffer, & Dave, 2010), and pulsatile (Akhavan et al., 2009; Bizhaem & Tabrizi, 2013) or secondary gas flows (Quevedo, Omosebi, & Pfeffer, 2010; Quevedo & Pfeffer, 2010). However, additional processing steps and units, as well as high operation costs are inevitable in this case. The second method is the addition of flow aids (Meyer & Zimmermann, 2004; Zhou & Li, 1999), either coarser or finer particles, to break up the agglomerates or reduce the adhesion forces by optimizing surface properties. But the bed segregation occurs possibly due to the difference in particle size and density, thus reducing the efficiency in improving flowability.

Although nanoparticles serving as the flow aids can be introduced to improve the flowability of cohesive powders, the improvement depends on how well they mix with each other.

* Corresponding author.
E-mail address: zhang-qiang@mails.tsinghua.edu.cn (Q. Zhang).

http://dx.doi.org/10.1016/j.partic.2016.09.001

Please cite this article in press as: Zhu, X., et al. Validation of surface coating with nanoparticles to improve the flowability of fine cohesive powders. *Particuology* (2016), http://dx.doi.org/10.1016/j.partic.2016.09.001

Nomenclature

A	Hamaker constant, J
Bo_g	Granular Bond number
Co	Granular cohesive number
Co_{A-C}	Critical granular cohesive number
Co'_{A-C}	Modified critical granular cohesive number
C_D	Drag coefficient
d	Diameter of guest particle, m
d_{ag}	Diameter of guest particle agglomerate, m
d_p	Particle diameter, m
D	Diameter of host particle, m
F_c	Interparticle adhesion force, N
F_d	Drag force, N
F_{vdw}	van der Waals force, N
N	Number of guest particles on the surface of each host particle
N_{ag}	Number of agglomerates on the surface of each host particle
ΔP	Pressure drop across fluidized bed
S	Cross-sectional area of fluidized bed
SAC	Surface area coverage, %
SAC^*	Actual surface area coverage, %
u	Superficial gas velocity, m/s
u_{mf}	Minimum fluidization velocity, m/s
u_t	Terminal velocity, m/s
W	Weight percentage of guest particle, wt.%
W_b	Buoyancy force, N
W_e	Effective weight, N
W_g	Gravity force, N
z_0	Minimum surface distance, m

Greek letters

ε	Voidage of solids bed
ε_{ag}	Voidage of guest particle agglomerate
ρ_d	Density of guest particle, kg/m^3
ρ_D	Density of host particle, kg/m^3
ρ_f	Gas density, kg/m^3
ρ_p	Particle density, kg/m^3
ϕ	Efficiency factor, %

Subscripts

d–D	(Attraction) between guest and host particles
D–D	(Attraction) between two host particles
guest–guest	Guest–guest contact
guest–host	Guest–host contact
host–host	Host–host contact

According to our previous experience, the nanoparticles are more easily to aggregate together than micron-sized cohesive powders because of their higher interparticle cohesion respect to gravity (Wang et al., 2007; Zhu, Zhang, Wang, & Wei, 2016). Some nanoparticles may even form a porous multi-stage agglomerate structure with the size up to several hundred microns (Huang, Wang, & Wei, 2008; Wang, Gu, Wei, & Wu, 2002). However, the particle agglomeration should be avoided for these nano-additives, given that it weakened their performance in reducing cohesiveness. Compared with simply blending the two kinds of powders together, coating the cohesive powders with nanoparticles can precisely deposit the nano-sized particles onto the surface of cohesive powders, reducing the interparticle adhesion force and improving the fluidization behavior more efficiently (Pfeffer, Dave, Wei, & Ramlakhan, 2001; Yang, Sliva, Banerjee, Dave, & Pfeffer, 2005). In addition, as the nanoparticles adhere to the surface of cohesive powders *via* van der Waals attraction, which is up to a million times the powder gravity (Kendall & Stainton, 2001), the tendency of particle segregation is effectively inhibited.

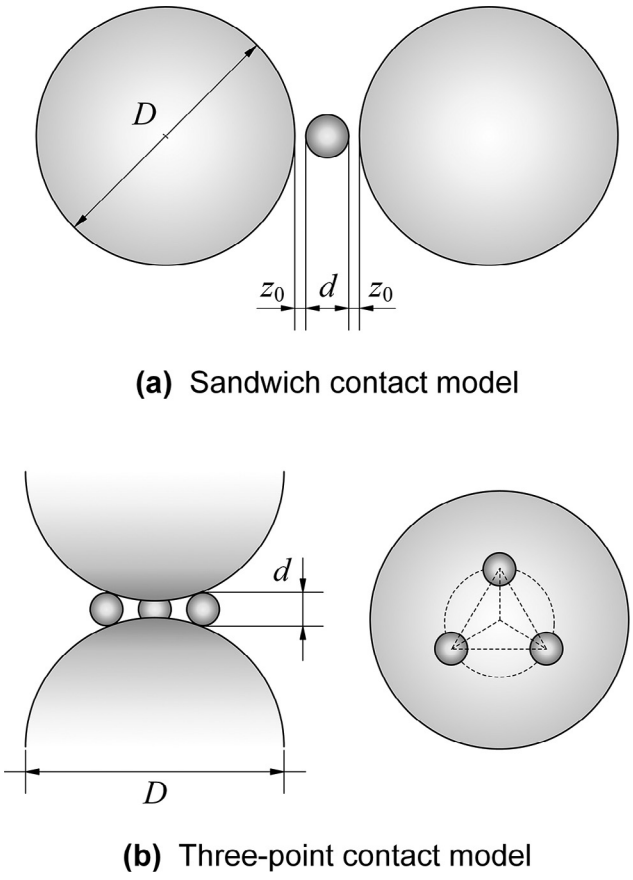

Fig. 1. Van der Waals force models of two coated particles: (a) sandwich contact model (Xie, 1997) and (b) three-point contact model (Chen et al., 2008).

In regard to the functional principles of nano-additives in improving powder flowability, it is widely accepted that van der Waals force decreases dramatically with increasing particle surface distance and dominates the interparticle forces for dry and neutral powders (Seville, Willett, & Knight, 2000; Visser, 1989). Therefore, most research groups believed that the nanoparticles acted as spacers, increased the surface distance between cohesive powders, and further reduced the interparticle adhesion force. To validate this theory, a series of research works have been conducted (Chen, Yang, Dave, & Pfeffer, 2008; Huang, Scicolone, Gurumuthy, & Davé, 2015; Xu, Zhang, & Zhu, 2009; Quintanilla, Valverde, & Castellanos, 2006). Especially, Xu et al. (2009) have successfully put this theory into practice by improving the flowability of powdered paints used in powder coating process (Huang, Zhang, & Zhu, 2010a). However, some researchers have questioned this mechanism and proposed different opinions, such as serving as lubricants to reduce the friction between cohesive powders (Podczeck & Mia, 1996; Utermann, Aurin, Benderoth, Fischer, & Schröter, 2011), and functioning as neutralizers of electrostatic charges (Dutta & Dullea, 1990).

Up to now, a number of van der Waals adhesion force models have been established to elucidate the role of nano-additives as spacers, such as sandwich contact model (Xie, 1997; Xu et al., 2009) only probing the particle size effect, and three-point contact model (Chen, Quintanilla, Yang, Valverde, & Dave, 2009; Chen et al., 2008) further taking the surface area coverage (SAC) into account (see Fig. 1). However, both the contact models assumed a homogeneous coating of the guest nanoparticles onto the host powders, neglecting the possible agglomeration of nano-

Please cite this article in press as: Zhu, X., et al. Validation of surface coating with nanoparticles to improve the flowability of fine cohesive powders. *Particuology* (2016), http://dx.doi.org/10.1016/j.partic.2016.09.001

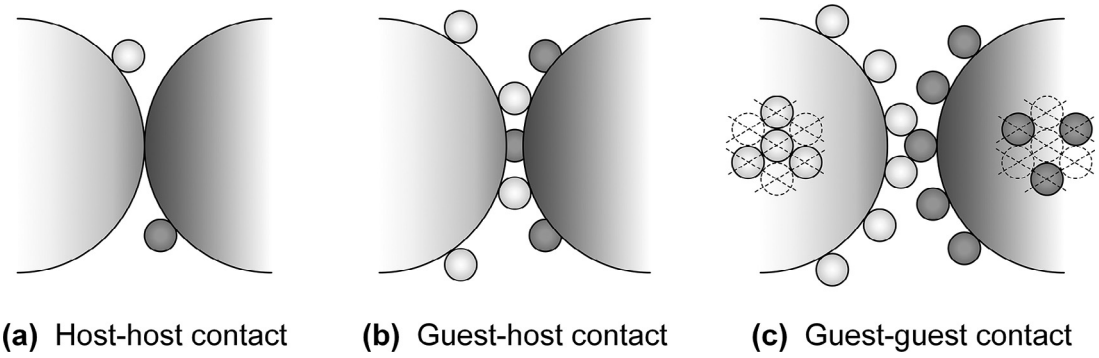

Fig. 2. Contact between two coated particles under different SACs (Chen et al., 2009).

additives. In this work, these interparticle force models were firstly reviewed and then extended to study the influence of the possible nano-additive agglomeration. Given that the majority of cohesive powders encountered in practice are irregularly shaped, an extreme case of cubic cohesive powders coated with silica nanoparticles was fabricated and tested for fluidization to validate the theory. Ultimately, based on force balance of a single particle, a semi-theoretical criterion was proposed to predict the fluidization behavior of coated cohesive powders, further guiding the practical application of such approach for improving powder flowability.

Theoretical

Adhesion force model of coated powders

To explain the fundamental roles of fine flow additives (i.e., guest particles), several models considering the effect of spacers on adhesion force between coarse host particles have been proposed previously (Tomas & Kleinschmidt, 2009). Both the sandwich (Fig. 1(a)) and three-point contact models (Fig. 1(b)) were the widely accepted cases, in which particles were assumed to be perfectly shaped spheres with smooth surfaces and their deformation was neglected (Chen et al., 2008; Xie, 1997). Here, these two models were primarily reviewed.

Sandwich contact model

Based on Rumpf's model (Rumpf, 1974) that interpreted the lower adhesion of rough surface by assuming the particle surface asperity as hemispherical, Xie (1997) firstly proposed the sandwich contact model. Subsequently, this model has been widely applied and extended to illustrate the function of guest particles introduced by Xu et al. (2009); Müller, Ruppel, Drexel, and Zimmermann (2008) and Kojima and Elliott (2013). As displayed in Fig. 1(a), an ultrafine guest particle is assumed to be centered between two coarse host particles in the sandwich contact model (Zimmermann, Eber, & Meyer, 2004). The van der Waals force F_{vdW} for this system is composed of two components, namely the attraction between the two host particles $F_{vdW,D-D}$ and the cohesion between the guest and host particles $F_{vdW,d-D}$, which is calculated as,

$$F_{vdW} = F_{vdW,D-D} + F_{vdW,d-D} = \frac{AD}{24(d+2z_0)^2} + \frac{AdD}{12z_0^2(d+D)}. \quad (1)$$

Herein, A is the Hamaker constant, z_0 is the minimum surface distance between two particles, d and D are the diameters of guest and host particles, respectively.

Three-point contact model

In a practical composite system with fine guest and coarse host particles, there are always many guest particles being involved in the contact, which induces a mechanically instable state otherwise. Moreover, the sandwich contact model mainly deals with the adhesion between two coarse particles with a centered fine particle, without taking the surface area coverage (SAC) of guest particles on host particles into account. To investigate the effect of *SAC* and approach the reality more closely, the three-point contact model assuming that two host particles are stably supported by three guest particles (see Fig. 1(b)) has been proposed (Chen et al., 2008). In this model, it is hypothesized that three guest particles are located on the peaks of an equilateral triangle, and the guest particles are individually and evenly distributed on the surface of host particles.

As illustrated in Fig. 2, the contact between two coated particles can be defined as three different stages depending on SAC, namely host–host, guest–host, and guest–guest contacts (Chen et al., 2009). When SAC is very low, the host particles contact directly (i.e., host–host contact), and the interparticle van der Waals force is the dominant interaction, which can be calculated as

$$F_{vdW,host-host} = \frac{AD}{24z_0^2}. \quad (2)$$

With increasing SAC up to a certain value, at which the two host particles start to depart from each other, the contact is transformed to guest–host pattern. At this time, the critical *SAC* is determined by Eq. (3) (Chen et al., 2009), and the decreasing adhesion force is estimated by Eq. (4) (Chen et al., 2008). Herein, Eqs. (3) and (4) are slightly different from the model deduced by Chen et al. (2008, 2009), for the reason that the guest particles are shared by the two neighboring host particles.

$$SAC_{guest-host} = \frac{0.604}{1+2(D/d)} \times 100\%, \quad (3)$$

$$F_{vdW,guest-host} = \frac{Ad}{4z_0^2} + \frac{A}{24D\left[\sqrt{(1+d/D)^2 - (0.604/SAC)(d/D)^2} - 1\right]^2}. \quad (4)$$

Ultimately, the guest–guest contact dominates the interaction with further increased SAC. Under the assumption that the guest particles are in hexagonal arrangement on host particle surface and the host particles are half coated with guest particles that well fit into the surface voids on neighboring particles, the transitional SAC from guest–host to guest–guest contact (i.e., $SAC_{quest-quest}$) is estimated to be 45.3% (Meyer & Zimmermann, 2004). In this case, the interparticle force can be computed as

$$F_{vdW,guest-guest} = \frac{Ad}{24z_0^2}. \quad (5)$$

Herein, we want to clarify that, the common sense that the smaller particles are more cohesive, is actually respect to the ratio of parti-

Please cite this article in press as: Zhu, X., et al. Validation of surface coating with nanoparticles to improve the flowability of fine cohesive powders. *Particuology* (2016), http://dx.doi.org/10.1016/j.partic.2016.09.001

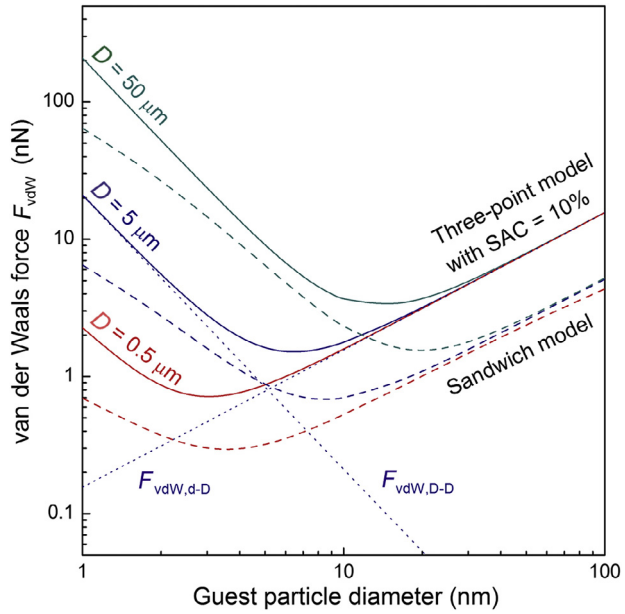

Fig. 3. Calculated van der Waals force against guest particle diameter based on three-point contact model (solid lines) and sandwich contact model (dash lines).

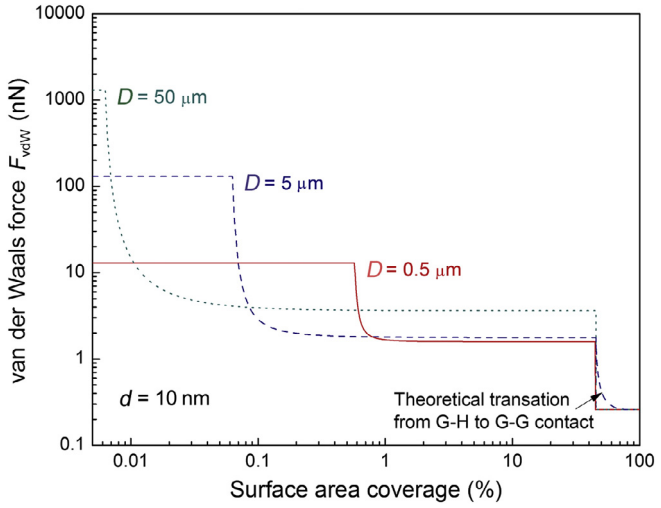

Fig. 4. Calculated van der Waals force against surface area coverage (*SAC*) based on three-point contact model (where the arrow points to the theoretical transition from guest–host to guest–guest contact which is omitted in this work).

cle cohesiveness to gravity (F_c/W_e). When omitting the electrostatic and capillary forces, the ratio of particle cohesiveness to gravity can be interpreted as $F_c/W_e \approx F_{vdw}/W_e$. Given that the effective gravity of a single particle in fluid equals $W_e = \pi(\rho_p - \rho_f)d_p{}^3/6$, F_c/W_e is propotional to $1/d_p{}^2$. That is the smaller the particle, the larger the F_c/W_e ratio. Moreover, due to the decreasing drag force between the particle and up-flowing fluid $F_d = C_D \frac{1}{2}\rho_f u^2 \frac{1}{4}\pi d_p^2$, the smaller particles are more difficult to be fluidized (Wang et al., 2007).

It should be noted that, both the presented three-point and sandwich contact models assume a homogeneous guest particle distribution. However, in practical mixing and coating processes, the guest particles are randomly distributed on the surface of host particles, and usually aggregate together due to the intensive interparticle interactions. Therefore, the impacts of particle agglomeration should be further investigated.

Model analysis of governing parameters

Based on the van der Waals force models reviewed above, both the effects of guest particle size and SAC on interparticle adhesion force, and the influence of guest particle agglomeration are systematically analyzed in this section. We want to clarify that, although the guest particle size and SAC have been analyzed by some previous studies, their effects are still discussed here to give the readers a full review. Moreover, none of the previous works has probed into the influence of the possible guest particle agglomeration.

Effect of guest particle size

The influence of guest particle size is primarily examined (Fig. 3) with fixed Hamaker constant $A = 10^{-19}$ J, minimum surface distance $z_0 = 0.4$ nm, and $SAC = 10\%$. For the host particle diameters ranging from 0.5 to 50 μm, the variation trend of van der Waals force with increasing guest particle size can be divided into three stages: the van der Waals force firstly decreases attributed to the increasing surface distance between host particles, then reaches a minimum value at a certain guest particle size (2–20 nm), and further increases when the attraction between the guest and host particles dominates the interaction. Precisely the two opposing components, namely decreasing host–host attraction ($F_{vdw,D-D}$) and increasing guest–host attraction ($F_{vdw,d-D}$) with the rise of guest particle size, result in the presence of the minimum adhesion force. Moreover, the impact of host particle size is also reflected by Fig. 3, which indicates that the interparticle adhesion force increases with the rise of host particle diameter. In addition, it should be noticed that, the van der Waals force calculated from the three-point contact model is larger than the sandwich model. This is primarily attributed to the fact that all interactions between the three guest particles and the two neighboring host particles are well considered in the three-point contact model.

Effect of surface area coverage

Fig. 4 plots van der Waals force versus SAC at a fixed guest particle size of $d = 10$ nm. When the SAC is low, guest particles distributed on host particles is sparse and the neighboring host particles directly contact with each other, namely the host–host contact. Therefore, the interparticle adhesion force remains constant. When the SAC increases up to $SAC_{quest-host}$ determined by Eq. (3), the distance between host particles started to increase because of surface-coated guest particles. Correspondingly, the adhesion force decreases sharply and then approaches constant at the guest–host contact stage. With increasing SAC up to a value at which monolayer distribution of guest particles on host particle surface is achieved, the guest–guest contact dominates the interaction and the adhesion force further decreases to some extent. For the host particles ranging from 0.5 to 50 μm, although the van der Waals force increases with the rise of host particle size, the transitional SAC from host–host to guest–host contact decreases. It is also indicated in Fig. 4 that the minimum SAC required to achieve a significant reduction in cohesiveness is about 1%, and the maximum cohesion reduction is achieved at the SAC higher than 45.3%.

The weight percentage of guest particles *W* and *SAC* defined in Eqs. (6) and (7), respectively, are related through the number of guest particles coated on the surface of each host particle, *N*. Accordingly, the *W* required to achieve a certain SAC can be determined.

$$W = \frac{Nd^3\rho_d}{D^3\rho_D + Nd^3\rho_d} \times 100\%, \tag{6}$$

$$SAC = \frac{N\left(\pi d^2/4\right)}{4\pi\left[(d+D)/2\right]^2} \times 100\% \approx \frac{Nd^2}{4D^2} \times 100\%. \tag{7}$$

Herein, ρ_d and ρ_D represent the density of guest and host particles, respectively.

Please cite this article in press as: Zhu, X., et al. Validation of surface coating with nanoparticles to improve the flowability of fine cohesive powders. Particuology (2016), http://dx.doi.org/10.1016/j.partic.2016.09.001

Effect of guest particle agglomeration

The guest particles inevitably aggregate together depending on material properties and coating processes in practical applications. Based on the solid volume balance of guest particles (Eq. (8)), the actual surface area coverage SAC^* can be deduced as Eq. (9), where N_{ag}, d_{ag}, and ε_{ag} represent the number, diameter, and void fraction of the quasi-spherical agglomerates, respectively.

$$N\frac{\pi}{6}d^3 = N_{ag}\frac{\pi}{6}d_{ag}^3\left(1-\varepsilon_{ag}\right), \tag{8}$$

$$SAC^* = \frac{N_{ag}d_{ag}^2}{4D^2}\times 100\% = \frac{d}{d_{ag}\left(1-\varepsilon_{ag}\right)}SAC. \tag{9}$$

Herein, a constant agglomerate void fraction of 0.5 close to the random packing limit of noncohesive powders is assumed (Huang et al., 2010a; Quintanilla et al., 2006). Then, it can be inferred by Eq. (9) that the SAC^* decreases linearly as a function of agglomeration ratio d/d_{ag}. Based on the hypothesis that the guest particle agglomerates are porous spheres and composed of the same material as host particles, the effects of agglomeration on interparticle cohesion are further investigated (Fig. 5), where a fixed host particle size $D = 5$ μm is used. Similar to the case of SAC, the variation trend of interparticle adhesion force with increasing weight percentage of guest particles is also divided into three stages (i.e., host–host, guest–host, and guest–guest contacts). However, as the agglomerate size increases up to 100 nm, the transition between each contact stage delays. Meanwhile, the van der Waals force increases due to the enhancing interaction between the agglomerates and host particles. Consequently, the effectiveness of nanoparticle coating to reduce the interparticle forces between micron-sized cohesive powders is weakened when the introduced nanoparticles aggregate together.

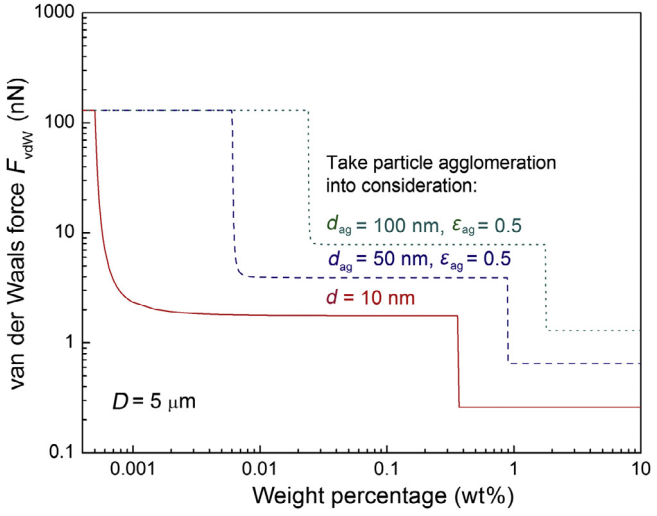

Fig. 5. Calculated van der Waals force against weight percentage of guest particles based on three-point contact model (where the dash lines further take the agglomeration of guest particles into consideration).

Experimental

Materials

To validate the theory, the cubic SAPO-34 zeolite with smooth surface (see the insets in Fig. 6) were employed as host particles in this work. The mean diameter of SAPO-34 powder determined by Malvern particle size analyzer (Mastersizer 2000, UK) was 20 mm, and the particle density was about 1500 kg/m^3. The microsized SAPO-34 zeolite is an industrial catalyst for conversion of methanol into ethylene and propylene, however, the well fluidization of 20 μm particles is very difficult. The spherical silica nanoparticles synthesized through the Stöber method (Stöber, Fink, & Bohn, 1968) served as the guest particles. Five monodisperse silica samples with different sizes (33, 59, 125, 257, and 602 nm) were prepared (Stöber et al., 1968), of which the particle density was around 2560 kg/m^3.

The particle coating process was carried out as follows. The SAPO-34 powder was firstly dispersed into fifteen times their weight of deionized water, and then a certain amount of silica particles were added under magnetic stirring. The as-prepared suspension was treated under sonication for 2.0 h, followed up by filtering and drying to obtain the coated samples.

The surface area coverage of coated SAPO-34 samples was determined by photo analysis of the scanning electron microscope (SEM, JEOL JSM 7401F, Japan) images. As displayed by the insets in Fig. 6, a relatively homogeneous and approximately monolayer dispersion of silica particles was attached on the surface of SAPO-34 powders. With the surface of coated powder being divided up, the number of

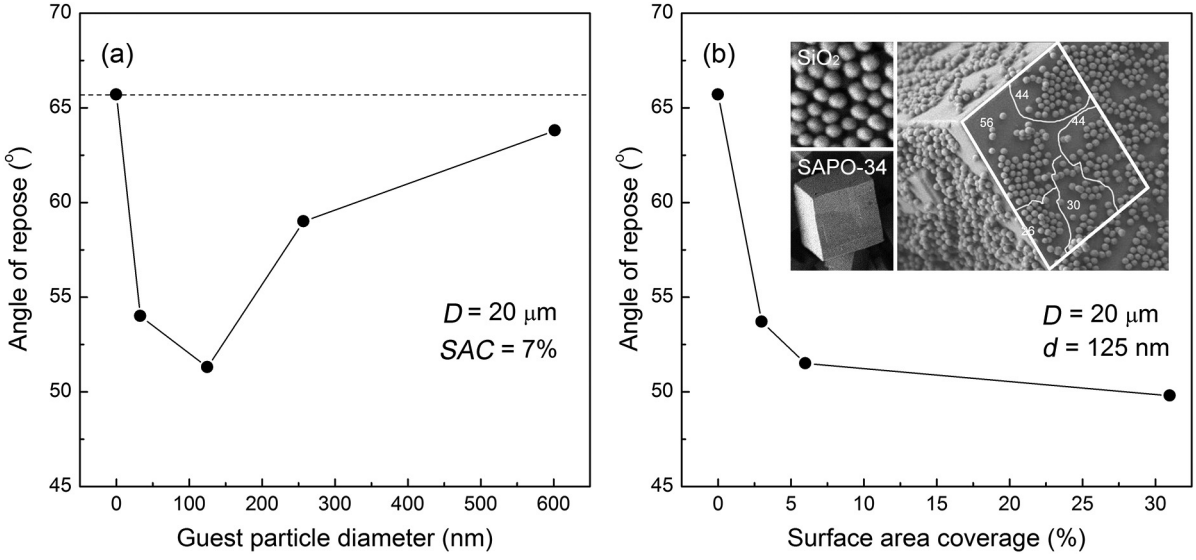

Fig. 6. Repose angles of coated SAPO-34 powders with various silica particle sizes (a) and surface area coverages (SACs) (b).

Please cite this article in press as: Zhu, X., et al. Validation of surface coating with nanoparticles to improve the flowability of fine cohesive powders. *Particuology* (2016), http://dx.doi.org/10.1016/j.partic.2016.09.001

silica particles in each division was counted manually. Considering the narrow size distribution of silica particles, their mean diameter combining the total quantity in defined regions were used to compute the surface area coverage, and at least five repeated measurements were conducted to obtain an average value.

Methods

The powder flowability has been evaluated by both the experiment of fluidization and test of static repose angle. Fluidization experiments were carried out in a column (55 mm inner-diameter and 1.0 m height) made of quartz to minimize static electricity. The fluidizing gas from the air compressor first passed through a silica filter drier to eliminate moisture, and then entered the fluidized bed via the bottom sintered porous plate. During each test, about 100 g powders were poured into the fluidization column. Afterwards, the gas velocity was increased gradually from 0 to 4 cm/s, with the pressure drop across the bed being measured by a U-shape manometer.

The angle of repose, directly related to the interparticle cohesiveness and friction, was also measured as an indicator of flowability. According to the method proposed by Santomaso, Lazzaro, and Canu (2003), the powder samples were fed through a sieve with an aperture size of 180 μm, and piled up as a cone on a circular plate. The angle between the cone edge and horizontal plate was determined to be the repose angle. To minimize the influence of falling height, the distance between final cone tip and sieve was maintained at less than 1.0 mm. Moreover, three circular plates with different sizes (12, 20, and 40 mm in diameter) were selected, and three repeated tests were conducted for each plate. Ultimately, an averaged value of the nine measurements was employed to characterize the sample.

Results and discussion

Flowability of coated cohesive powders

In the most reported literature, the spherical host and guest particles were applied to investigate the role of flow additives. However, the majority of cohesive powders encountered in practice are irregularly shaped. Therefore, whether the nano-sized additives is still effective in improving the flowability of cohesive powders with irregular shapes becomes a key issue. In this contribution, the cubic SAPO-34 powders have been tested as an extreme case for host particle, with silica nanospheres serving as the guest particle. Given the fact that the dynamic process is best suited for evaluating fluidization performance and the static technique is much better for predicting particle agglomeration (Krantz, Zhang, & Zhu, 2009), both dynamic and static characterizations (i.e., fluidization experiment and repose angle test) have been carried out to validate the theory effectiveness for irregularly shaped cohesive powders.

Repose angle tests

The angle between the horizontal and a pile of powder generated by pouring, namely the static angle of repose, is widely used as an indicator for powder cohesiveness and flowability. Due to the strong interparticle adhesion forces, the repose angle of cohesive powders is much larger than the noncohesive ones. De Jong, Hoffmann, and Finkers (1999) have provided an indication of powder flow behavior in regard to the repose angle. They termed the powders with repose angles in the ranges of >60°, 45°–60°, 30°–45°, and 10°–30° as non-flowing, fairly free-flowing, free-flowing, and excellent flowing, respectively.

In accordance with the above model, both the effects of additive size and SAC on improving the powder flowability have been investigated experimentally. For most of the coated samples, the silica spheres were almost homogeneous and monolayer dispersed on the surface of cubic SAPO-34 powders (see the insets in Fig. 6). Fig. 6(a) plots the test results of repose angle against guest particle diameter, under fixed host particle size $D = 20$ μm and $SAC = 7\%$. The repose angle of pristine host particles was up to 66°, demonstrating a cohesive and hardly-flowing characteristic (De Jong et al., 1999). Upon the introduction of guest particles, the repose angle of coated host powders decreased to a minimum value of 51° at a guest particle size $d = 125$ nm, indicating an improved flow property. However, the repose angle became large instead with further increasing guest particle diameter, which was attributed to the dominating attraction between the guest and host particles according to the previous theoretical analysis.

The influence of SAC is examined in Fig. 6(b) at fixed host and guest particle sizes $D = 20$ μm and $d = 125$ nm. The variation trend of repose angle with SAC was fully consistent with that of interparticle adhesion forces discussed above. For the pristine host particles directly contacting with each other, a large repose angle of 66° was achieved due to the intensive interparticle cohesion. As the SAC increased to 6%, the surface distance between neighboring host particles was enlarged by the introduced guest particles, consequently resulting in a sharp decreasing repose angle to 52°. With further increasing SAC up to 31%, the repose angle decreased gradually and then remained relatively constant when the guest-host attraction dominated the interaction.

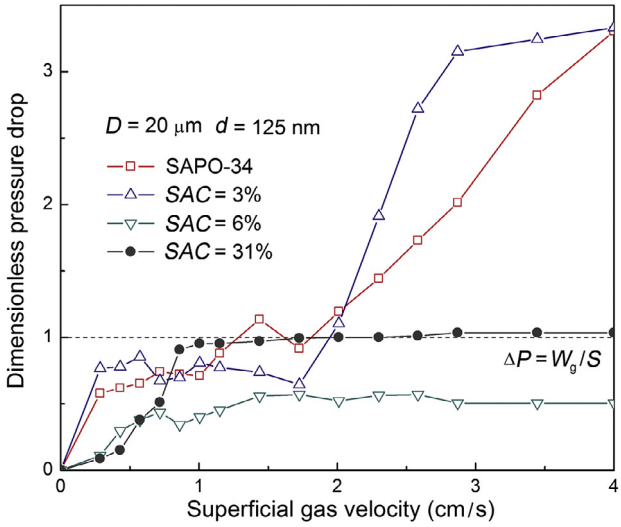

Fig. 7. Fluidization curves of coated SAPO-34 powders with different SACs.

Fluidization experiments

Fluidization experiments of the coated samples with different SACs have also been carried out. Fig. 7 plots the dimensionless bed pressure drop against the superficial gas velocity. Herein, the dimensionless pressure drop is defined as the pressure drop across the whole bed (ΔP) divided by the weight of loaded powder (W_g) per unit cross-sectional area (S). Theoretically, when the particles loaded in the bed are entirely fluidized, the dimensionless pressure drop attains unity and remains constant with further increasing gas velocity. As for the pristine SAPO-34 powder and the coated samples with a SAC of 3%, the pressure drop increased continuously with the rise of gas velocity. Meanwhile, typical Group C fluidization behavior, including gas channeling, powder plugging, and large agglomerates at bed bottom, was observed. Due to the strong cohesiveness of the powder and a possible pressure loss through the bed full of powder plugs and agglomerates, the dimensionless pressure drop was even increased up to three. When SAC increased to 6%, a plateau of dimensionless pressure drop around 0.5 was obtained

Please cite this article in press as: Zhu, X., et al. Validation of surface coating with nanoparticles to improve the flowability of fine cohesive powders. *Particuology* (2016), http://dx.doi.org/10.1016/j.partic.2016.09.001

when the superficial gas velocity was higher than 1.5 cm/s, indicating partial of the bed had been fluidized. With further increasing SAC up to 31%, the pressure drop plateau approached unity and the bed was fully fluidized at a minimum fluidization velocity of 1.0 cm/s, fully demonstrating the effectiveness of nanoparticle coating in improving the flowability of cohesive powders.

In summary, the repose angle of cubic SAPO-34 powder decreased obviously and the fluidization behavior was improved with the introduction of silica nanospheres. Both the results of static and dynamic tests indicated that surface coating with nanoparticles was also effective in improving the flow properties for the irregularly shaped powders.

Criterion for predicting powder flowability

The powder flow behavior is significantly influenced by the interparticle forces. For instance, the Group C powders of which the interparticle adhesion force is much larger than the gravity, usually form cracks, channels, or even lift as slugs during fluidization. In contrast, the Group A powders with much lower adhesion force can be fluidized individually, and the uniform flow property facilities much better heat and mass transfer. Although surface coating with nanoparticles can improve the flowability of Group C cohesive powders, the quantitative model to predict the flow behavior is still lacking. In this section, through force analysis of a single particle, the mechanism of surface modification to reduce interparticle cohesiveness is further discussed, and a criterion for predicting the fluidization behavior of coated cohesive powders is developed.

Force analysis of single particle

For an individual particle in infinite fluid at terminal velocity u_t, the drag force is balanced by the net force of gravity and buoyancy, that is,

$$C_D \frac{\rho_f u_t^2}{2} \frac{\pi D^2}{4} = \frac{\pi}{6} D^3 (\rho_D - \rho_f) g, \tag{10}$$

where C_D is the drag coefficient, and ρ_f is the gas density. Meanwhile, a granular cohesive number Co is defined as the ratio of interparticle adhesion force F_c to net force of gravity and buoyancy:

$$Co = \frac{F_c}{\frac{\pi}{6} D^3 (\rho_D - \rho_f) g}. \tag{11}$$

For an individual particle in a fluidized bed of voidage ε, the drag force exerted on it F_d is $\varepsilon^{-4.8}$ times that acting on a single isolated particle for the same superficial gas velocity u (Khan & Richardson, 1990), that is,

$$F_d = C_D \frac{\rho_f u^2}{2} \frac{\pi D^2}{4} \varepsilon^{-4.8}. \tag{12}$$

The effective weight of a single particle W_e in the bed equals its gravity force W_g minus the buoyancy force W_b,

$$\begin{aligned} W_e &= W_g - W_b \\ &= \frac{\pi}{6} D^3 \rho_D g - \frac{\pi}{6} D^3 [\varepsilon \rho_f + (1-\varepsilon) \rho_D] g \\ &= \frac{\pi}{6} D^3 (\rho_D - \rho_f) g \varepsilon. \end{aligned} \tag{13}$$

When the solids bed is subjected to fluidizing gas, the forces acted on an individual particle include the drag force, the gravity and buoyancy force, and the adhesion force (see Fig. 8). The regime of fluidization is reasonably defined by the superficial gas velocity u within the range of minimum fluidization velocity u_{mf} and terminal velocity u_t (i.e., $u_{mf} \le u \le u_t$) (Molerus, 1982). If the maximal drag force (when $u = u_t$) exerted by the percolating gas within the regime of fluidization exceeds the sum of adhesion force plus effective particle weight, the fixed bed structure is broken up and the particles are fluidized individually. If not, the solids bed remains fixed and the limit of fluidization is reached (here the agglomerate fluidization is omitted). Therefore, the transition equation between Group A and Group C powders can be expressed as follows (Qian et al., 2001):

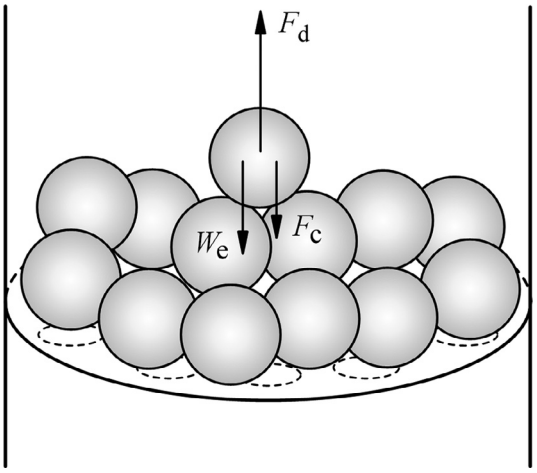

Fig. 8. Force analysis for a single particle in fluidized bed.

$$F_d|_{u=u_t} = W_e + F_c. \tag{14}$$

Substituting Eqs. (10)–(13) into Eq. (14), the transition equation in terms of the maximal drag force is transformed to the expression in terms of critical granular cohesive number Co_{A-C}:

$$Co_{A-C} = \varepsilon^{-4.8} - \varepsilon. \tag{15}$$

Herein, ε is the voidage of the solids bed before fluidization, which can be estimated using a recently developed correlation (Capece et al., 2014) between the bed voidage ε and the granular Bond number Bo_g (which is the ratio of cohesion to gravity F_c/W_g), as given by:

$$\varepsilon = 0.44{+}0.56\exp\left(-3.09 {Bo_g}^{-0.224}\right). \tag{16}$$

By now, a semi-theoretical criterion is set up to predict the powder flowability. As for the cohesive powders with surface coated nanoparticles, the interparticle adhesion force (here, both electrostatic and capillary force are omitted) can be calculated based on the three-point contact model as given by Eqs. (2)–(5). Then, both Bo_g and Co are computed according to their definitions, and Co_{A-C} is further determined by Eqs. (15) and (16). Through the comparison between Co and Co_{A-C}, the flowability of coated cohesive powders is able to be predicted. In the case of $Co < Co_{A-C}$, the coated powders can be fluidized smoothly, behaving like Group A particles. While for $Co > Co_{A-C}$, the coated powders cannot be fluidized individually, still behave as Group C particles.

Validation and modification of the criterion

To verify the reliability of the proposed criterion for predicting powder flowability after being coated with nanoparticles, experimental data from both this work and the literature (as listed in Table 1) concerning the fluidization of coated cohesive powders were used, with D = 3–20 μm, d = 7–125 nm, and SAC = 0–100%. Fig. 9(a) plots Co of these data versus Co_{A-C} determined by Eqs. (15) and (16). The solid line in Fig. 9(a) denotes $Co = Co_{A-C}$, therefore, the upper left region (gray area) indicates the results of $Co < Co_{A-C}$, and the lower right region (white area) presents the results of $Co > Co_{A-C}$. Moreover, the solid symbols indicate that the powders are fully fluidized during fluidization experiments (i.e., a plateau of dimensionless bed pressure drop approaching unity is obtained with increasing gas velocity), while the hollow symbols represent

Please cite this article in press as: Zhu, X., et al. Validation of surface coating with nanoparticles to improve the flowability of fine cohesive powders. *Particuology* (2016), http://dx.doi.org/10.1016/j.partic.2016.09.001

Table 1
Properties of host and guest particles used from the reported literature and this study.

Author	Host particle			Guest particle			SAC (%)
	Material	D (μm)	ρ_D (kg/m^3)	Material	d (nm)	ρ_d (kg/m^3)	
Chen et al. (2008)	Cornstarch	15	1550	SiO_2	7–100	2650	1–100
	Al_2O_3	3–14	2700				100
Huang et al. (2010a, 2010b)	Polyurethane	19	1570	SiO_2	12	2000	8–100
				Al_2O_3	13	3270	6–100
				TiO_2	40	3800	2–60
This study	SAPO-34	20	1500	SiO_2	33–602	2560	3–31

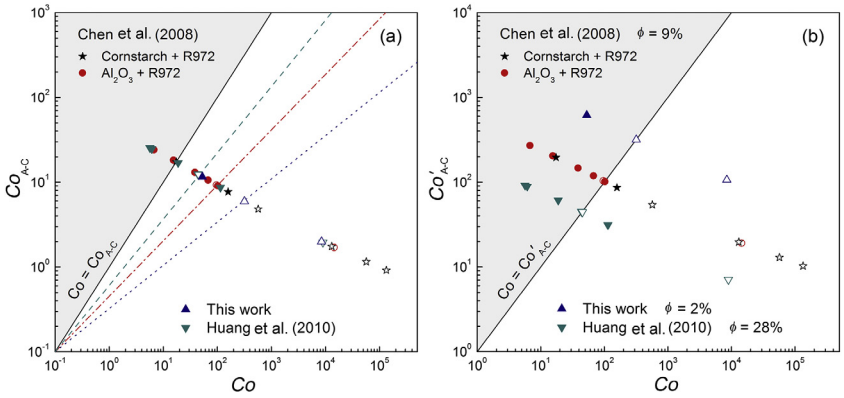

Fig. 9. Transition between Group A and Group C flow characteristics based on granular cohesive number before (a) and after (b) modification (where solid symbols indicate that the powders have been fully fluidized during experiment, and hollow symbols represent that the solids bed could not be fluidized entirely).

that the solids bed can not be fluidized entirely (i.e., the pressure drop plateau is less than unity or no plateau is detected).

As displayed in Fig. 9(a), all symbols in the region above the $Co = Co_{A-C}$ solid line are solid, demonstrating the coated powders have been fluidized experimentally. However, besides the hollow symbols which represent that the bed has not been fully fluidized, a number of solid symbols are also observed in the region below the $Co = Co_{A-C}$ line. This result indicates that the semi-theoretical criterion proposed to predict the flowability of coated cohesive powders deviates from the actual boundary (see the dash lines in Fig. 9(a)). On one hand, this can be attributed to the agglomerate fluidization of the cohesive powders, which reduces the interparticle adhesion force and Co, thus shifting the realistic features toward upper left region. On the other hand, neglecting the difference between the estimated interparticle adhesion force (based on the three-point contact model) and the practical cohesive force may also result in the deviation. Although some samples with $Co > Co_{A-C}$ can be fluidized for the reasons given above, the conclusion that the coated powders could be fluidized when $Co < Co_{A-C}$ is still valid. In spite of a high SAC and an optimal additive size that are required to guarantee $Co < Co_{A-C}$, namely smooth fluidization behavior, the critical granular cohesive number Co_{A-C} is still a useful index for practical applications.

When neglecting agglomerate fluidization, the inaccuracy of the proposed semi-theoretical criterion may be ascribed to the deviation of the estimated interparticle adhesion forces from their actual values. In the three-point contact model, it is assumed that the particles are perfectly shaped spheres with smooth surfaces. However, the available data concerning the fluidization of coated cohesive powders mostly used irregularly shaped particles with rough surfaces. Given that both the deviation of particle shape from sphere and the asperity on particle surface reduced the interparticle adhesion force, an efficiency factor ϕ indicating the ratio of actual adhesion force to its predicted value is introduced to correct the interparticle cohesiveness (see Eq. (17)). Accordingly, the modified critical granular cohesive number Co'_{A-C} can be calculated as Eq. (18).

$$F_d|_{u=u_t} = W_e + \phi F_c, \tag{17}$$

$$Co'_{A-C} = \left(\varepsilon^{-4.8} - \varepsilon\right)/\phi. \tag{18}$$

The comparison between Co and the corrected boundary Co'_{A-C} is displayed in Fig. 9(b). After the modification, the flowability of coated cohesive powders from both this work and the literature is well predicted. It should be noted here that, distinct efficiency factor values have been assigned to the different studies. The efficiency factor generally decreases with reducing sphericity of the investigated host particles, for instance, the cubic SAPO-34 powders used in this work exhibit the lowest ϕ value of 2%. Although the revised criterion gives a relatively satisfactory prediction of the coated-powder flowability, the modification is confined to every individual work, and additional experimental data are still necessary to obtain an widely applicable standard.

Conclusions

Based on the previously proposed van der Waals adhesion force models, the mechanism of nanoparticle coating in reducing the cohesiveness and improving the flowability of fine cohesive powders was revisited, and the influence of possible agglomeration of nano-additives was also investigated. Model analysis of the governing parameters indicated that an optimal nanoparticle size around 10 nm and a minimum SAC ca. 1% was required to achieve significant cohesiveness reduction for the cohesive powders of 0.5–50 μm diameters. To verify the effectiveness of nano-additives in improving the flowability of irregularly shaped cohesive powders, the cubic SAPO-34 particles were tested as an extreme case. Both static and dynamic characterizations were conducted to evaluate the powder flowability. When coating with silica nanoparticles of an optimal size and sufficiently high SAC, the repose angle of the

Please cite this article in press as: Zhu, X., et al. Validation of surface coating with nanoparticles to improve the flowability of fine cohesive powders. *Particuology* (2016), http://dx.doi.org/10.1016/j.partic.2016.09.001

coated cubic SAPO-34 powders decreased from 66° to 50°, directly validating the effectiveness of the theory. As for the fluidization experiments, the bed of coated SAPO-34 powders was fully fluidized with increasing SAC up to 31%.

Furthermore, through force analysis of a single particle, a semi-theoretical criterion was proposed to predict the flow behavior of coated cohesive powders. Due to the difference between estimated interparticle forces and their actual values, the criterion deviates to some extent from the results of this work and the literature concerning the fluidization of coated powders. Although additional data are required to achieve a general applicable criterion, it can still be concluded that, the coated cohesive powders are able to be fluidized entirely when the granular cohesive number *Co* is less than the critical value Co_{A-C}. However, an efficient method to take into account the agglomerate of nanoparticles in practical coating processes is still in need.

Acknowledgments

The authors acknowledge the financial supports provided by the National Key Research and Development Program (No. 2016YFA0200101), the National Natural Science Foundation of China (Nos. 21306102 and 21422604) and the China Postdoctoral Science Foundation (No. 2015M571049).

References

Akhavan, A., van Ommen, J. R., Nijenhuis, J., Wang, X. S., Coppens, M. O., & Rhodes, M. J. (2009). Improved drying in a pulsation-assisted fluidized bed. *Industrial & Engineering Chemistry Research*, *48*, 302–309.

Bizhaem, H. K., & Tabrizi, H. B. (2013). Experimental study on hydrodynamic characteristics of gas-solid pulsed fluidized bed. *Powder Technology*, *237*, 14–23.

Capece, M., Huang, Z., To, D., Aloia, M., Muchira, C., Davé, R., et al. (2014). Prediction of porosity from particle scale interactions: Surface modification of fine cohesive powders. *Powder Technology*, *254*, 103–113.

Chen, Y., Quintanilla, M. A., Yang, J., Valverde, J. M., & Dave, R. N. (2009). Pull-off force of coated fine powders under small consolidation. *Physical Review E*, *79*, 041305.

Chen, Y., Yang, J., Dave, R. N., & Pfeffer, R. (2008). Fluidization of coated group C powders. *AIChE Journal*, *54*, 104–121.

De Jong, J. A., Hoffmann, A. C., & Finkers, J. (1999). Properly determine powder flowability to maximize plant output. *Chemical Engineering Progress*, *95*, 25–34.

Dutta, A., & Dullea, L. (1990). A comparative evaluation of negatively and positively charged submicron particles as flow conditioners for a cohesive powder. *AIChE Symposium Series*, *86*, 26–40.

Geldart, D. (1973). Types of gas fluidization. *Powder Technology*, *7*, 285–292.

Guo, Q. J., Liu, H., Shen, W. Z., Yan, X. H., & Jia, R. G. (2006). Influence of sound wave characteristics on fluidization behaviors of ultrafine particles. *Chemical Engineering Journal*, *119*, 1–9.

Huang, C., Wang, Y., & Wei, F. (2008). Solids mixing behavior in a nano-agglomerate fluidized bed. *Powder Technology*, *182*, 334–341.

Huang, Q., Zhang, H., & Zhu, J. (2009). Experimental study on fluidization of fine powders in rotating drums with various wall friction and baffled rotating drums. *Chemical Engineering Science*, *64*, 2234–2244.

Huang, Q., Zhang, H., & Zhu, J. (2010a). Flow properties of fine powders in powder coating. *Particuology*, *8*, 19–27.

Huang, Q., Zhang, H., & Zhu, J. (2010b). Onset of an innovative gasless fluidized bed-comparative study on the fluidization of fine powders in a rotating drum and a traditional fluidized bed. *Chemical Engineering Science*, *65*, 1261–1273.

Huang, Z., Scicolone, J. V., Gurumuthy, L., & Davé, R. N. (2015). Flow and bulk density enhancements of pharmaceutical powders using a conical screen mill: A continuous dry coating device. *Chemical Engineering Science*, *125*, 209–224.

Kaliyaperumal, S., Barghi, S., Briens, L., Rohani, S., & Zhu, J. (2011). Fluidization of nano and sub-micron powders using mechanical vibration. *Particuology*, *9*, 279–287.

Kendall, K., & Stainton, C. (2001). Adhesion and aggregation of fine particles. *Powder Technology*, *121*, 223–229.

Khan, A., & Richardson, J. (1990). Pressure gradient and friction factor for sedimentation and fluidisation of uniform spheres in liquids. *Chemical Engineering Science*, *45*, 255–265.

Kojima, T., & Elliott, J. A. (2013). Effect of silica nanoparticles on the bulk flow properties of fine cohesive powders. *Chemical Engineering Science*, *101*, 315–328.

Krantz, M., Zhang, H., & Zhu, J. (2009). Characterization of powder flow: Static and dynamic testing. *Powder Technology*, *194*, 239–245.

Lepek, D., Valverde, J. M., Pfeffer, R., & Dave, R. N. (2010). Enhanced nanofluidization by alternating electric fields. *AIChE Journal*, *56*, 54–65.

Liu, H., Guo, Q. J., & Chen, S. A. (2007). Sound-assisted fluidization of SiO_2 nanoparticles with different surface properties. *Industrial & Engineering Chemistry Research*, *46*, 1345–1349.

Müller, A.-K., Ruppel, J., Drexel, C.-P., & Zimmermann, I. (2008). Precipitated silica as flow regulator. *European Journal of Pharmaceutical Sciences*, *34*, 303–308.

Meyer, K., & Zimmermann, I. (2004). Effect of glidants in binary powder mixtures. *Powder Technology*, *139*, 40–54.

Molerus, O. (1982). Interpretation of Geldart's type A, B, C and D powders by taking into account interparticle cohesion forces. *Powder Technology*, *33*, 81–87.

Nam, C. H., Pfeffer, R., Dave, R. N., & Sundaresan, S. (2004). Aerated vibrofluidization of silica nanoparticles. *AIChE Journal*, *50*, 1776–1785.

Pfeffer, R., Dave, R. N., Wei, D., & Ramlakhan, M. (2001). Synthesis of engineered particulates with tailored properties using dry particle coating. *Powder Technology*, *117*, 40–67.

Podczeck, F., & Mia, Y. (1996). The influence of particle size and shape on the angle of internal friction and the flow factor of unlubricated and lubricated powders. *International Journal of Pharmaceutics*, *144*, 187–194.

Qian, G. H., Bagyi, I., Burdick, I. W., Pfeffer, R., Shaw, H., & Stevens, J. G. (2001). Gas–solid fluidization in a centrifugal field. *AIChE Journal*, *47*, 1022–1034.

Quevedo, J. A., Omosebi, A., & Pfeffer, R. (2010). Fluidization enhancement of agglomerates of metal oxide nanopowders by microjets. *AIChE Journal*, *56*, 1456–1468.

Quevedo, J. A., & Pfeffer, R. (2010). In situ seasurements of gas gluidized nanoagglomerates. *Industrial & Engineering Chemistry Research*, *49*, 5263–5269.

Quintanilla, M., Valverde, J., & Castellanos, A. (2006). Adhesion force between fine particles with controlled surface properties. *AIChE Journal*, *52*, 1715–1728.

Rumpf, H. (1974). Die wissenschaft des agglomerierens. *Chemie Ingenieur Technik*, *46*, 1–11.

Santomaso, A., Lazzaro, P., & Canu, P. (2003). Powder flowability and density ratios: The impact of granules packing. *Chemical Engineering Science*, *58*, 2857–2874.

Seville, J., Willett, C., & Knight, P. (2000). Interparticle forces in fluidisation: A review. *Powder Technology*, *113*, 261–268.

Stöber, W., Fink, A., & Bohn, E. (1968). Controlled growth of monodisperse silica spheres in the micron size range. *Journal of Colloid and Interface Science*, *26*, 62–69.

Tomas, J., & Kleinschmidt, S. (2009). Improvement of flowability of fine cohesive powders by flow additives. *Chemical Engineering & Technology*, *32*, 1470–1483.

Utermann, S., Aurin, P., Benderoth, M., Fischer, C., & Schröter, M. (2011). Tailoring the frictional properties of granular media. *Physical Review E*, *84*, 031306.

van Ommen, J. R., Valverde, J. M., & Pfeffer, R. (2012). Fluidization of nanopowders: A review. *Journal of Nanoparticle Research*, *14*, 1–29.

Visser, J. (1989). Van der Waals and other cohesive forces affecting powder fluidization. *Powder Technology*, *58*, 1–10.

Wang, F.-J., Zhu, J.-X., & Beeckmans, J. (2000). Pressure gradient and particle adhesion in the pneumatic transport of cohesive fine powders. *International Journal of Multiphase Flow*, *26*, 245–265.

Wang, Y., Cheng, Y., Jin, Y., & Bi, H. T. (2007). On impacts of solid properties and operating conditions on the performance of gas-solid fluidization systems. *Powder Technology*, *172*, 167–176.

Wang, Y., Gu, G., Wei, F., & Wu, J. (2002). Fluidization and agglomerate structure of SiO_2 nanoparticles. *Powder Technology*, *124*, 152–159.

Xie, H.-Y. (1997). The role of interparticle forces in the fluidization of fine particles. *Powder Technology*, *94*, 99–108.

Xu, C., Cheng, Y., & Zhu, J. (2006). Fluidization of fine particles in a sound field and identification of group C/A particles using acoustic waves. *Powder Technology*, *161*, 227–234.

Xu, C., & Zhu, J. (2005). Experimental and theoretical study on the agglomeration arising from fluidization of cohesive particles-effects of mechanical vibration. *Chemical Engineering Science*, *60*, 6529–6541.

Xu, C., & Zhu, J. (2006). Parametric study of fine particle fluidization under mechanical vibration. *Powder Technology*, *161*, 135–144.

Xu, C. C., Zhang, H., & Zhu, J. (2009). Improving flowability of cohesive particles by partial coating on the surfaces. *The Canadian Journal of Chemical Engineering*, *87*, 403–414.

Yang, J., Sliva, A., Banerjee, A., Dave, R. N., & Pfeffer, R. (2005). Dry particle coating for improving the flowability of cohesive powders. *Powder Technology*, *158*, 21–33.

Yu, Q., Dave, R. N., Zhu, C., Quevedo, J. A., & Pfeffer, R. (2005). Enhanced fluidization of nanoparticles in an oscillating magnetic field. *AIChE Journal*, *51*, 1971–1979.

Zhou, T., & Li, H. (1999). Effects of adding different size particles on fluidization of cohesive particles. *Powder Technology*, *102*, 215–220.

Zhu, X., Zhang, Q., Wang, Y., & Wei, F. (2016). Review on the nanoparticle fluidization science and technology. *Chinese Journal of Chemical Engineering*, *24*, 9–22.

Zimmermann, I., Eber, M., & Meyer, K. (2004). Nanomaterials as flow regulators in dry powders. *Zeitschrift Fur Physikalische Chemie*, *218*, 51–102.

Please cite this article in press as: Zhu, X., et al. Validation of surface coating with nanoparticles to improve the flowability of fine cohesive powders. *Particuology* (2016), http://dx.doi.org/10.1016/j.partic.2016.09.001